An Algorithm for Tracking Eyes of Tropical Cyclones

Pao-Liang Chang[1] Ben Jong-Dao Jou[2] Jian Zhang[3]

[1] Meteologogical Satellite Center, Central Weather Bureau

[2]Department of Atmospheric Sciences, National Taiwan University

[3]Cooperative Institute for Mesoscale Meteorological Studies, The University of Oklahoma, USA

Abstract

A Tropical Cyclone (TC) Eye Tracking (TCET) algorithm is presented in this study to objectively identify and track the eye and center of a tropical cyclone using radar reflectivity data. Twelve typhoon cases were studied for evaluating the TCET algorithm. Results show that the TCET can track TC centers for several hours. The longest tracking time is about 35 hours. Eye locations estimated from different radars showed consistency with a mean distance bias of about 3.5 km and a standard deviation of about 1.5 km. The TCET analysis shows decreasing eye radius as TCs approach land, especially within 50 km of the coastline.

The TCET algorithm is computationally efficient and can be automated by using the TC center in the previous volume or the estimated center from satellite images as an initial guess. The TCET may not accurately find the TC center when a TC is weak or does not have an enclosed eyewall or have highly non-circular eyes. However, it is still suitable for operational implementation and provides high spatial and temporal resolution information for TC centers and eye radii, especially for intense TCs.

1. Introduction

The eye and eyewall are signature characteristics of a mature Tropical Cyclone (TC), and knowing their locations is crucial for operational weather forecasts near and during TC landfalls. Several methods have been developed to identify typhoon centers using Doppler radar velocity and reflectivity fields (e.g. Lee and Marks 2000; Griffin et al. 1992). The eye region is often characterized with weak or no echoes and surrounded by a more or less complete wall of deep convection where the extreme tangential and ascending wind velocities are located (Willoughby 1998; Blackwell 2000). According to the thermodynamic characteristics in the eye of a mature TC (Willoughby 1998), the eye can be regarded as a closed area with weak or no radar reflectivity. In past studies, Parrish et al. (1984), and Muramatsu (1986) manually tracked reflectivity echoes and reported rapid cyclonic movement around the eye. And TC centers are often subjectively identified as the centroid of an oval-shaped weak echo or echo-free area (Griffin et al. 1992).

Based on Doppler velocity data, Wood and Brown (1992) developed a geometric method for determining the circulation centers of Rankine-like vortices. The method provided a direct estimation of the circulation strength, radius of maximum wind (RMW), and the center location of a TC from Doppler radar data, and could be applied in an operational environment. However, it was highly affected by the asymmetry of circulations and strong mean flows across the vortex. Marks et al. (1992) used the "simplex" algorithm to find the center that maximizes tangential circulations encompassing the observed RMW at different altitudes. They found that the center was 3-6 km to the right of that determined objectively from the flight-level inertial navigation system (INS) winds. Further, Lee and Marks (2000) used the "simplex" concept and proposed an algorithm based on ground-based velocity-track-display (GBVTD) (Lee et al. 1999) wind retrieval technique to estimate vorticity centers by maximizing GBVTD's retrieved mean tangential wind. The GBVTD- simplex can be automated such that the initial guess is assigned as the vorticity center in the previous volume or estimated from the method outlined in Wood and Brown (1992).

The Tropical Cyclone Eye Tracking (TCET) algorithm proposed in this study can potentially improve the objective identification of TC eye and center locations by using an iterative procedure with multiple parameters that define physical structure of TC eyes. The TCET algorithm is presented in section 2. Section 3 shows the TCET results and comparisons among different radars. A summary will be given in section 4.

2. Data and methodology

The strong winds and heavy rainfall associated with a TC lead to significant losses of property and human lives each year in Taiwan, even if the storm does not make landfall (Wu et al. 2002). For improving the mesoscale observations of typhoons, the Central Weather Bureau (CWB) of Taiwan implemented a Doppler radar network around Taiwan Island between 1996 and 2001. These radars provide frequent information such as TC positions, tracks, and intensity changes as typhoons approach Taiwan. They also provide details of mesoscale circulations and precipitation structure in the inner core and rainbands of typhoons as they impact Taiwan.

Different from Griffin et al. 1992, a TC center in the TCET algorithm is defined as the geometric center of the radar eye region rather than the inner edge of the eyewall. Furthermore, a circular shape is assumed in TCET for the eye of a tropical cyclone based on common observations (Chang et al. 2008).

1) Find an initial guess of the typhoon center (X^0, Y^0) in a Cartesian coordinate with the origin at the radar site, the eye radius (R_0) and weak echo threshold (Z_0). Here, X^0, Y^0, Z_0 and R_0 can be determined subjectively with satellite or radar images or by taking the values found in the previous volume.
2) In any given (m^{th}) iteration, the estimated TC center at the lowest PPI is defined as

$$X^m = \frac{1}{A}\int X dA \ , \ Y^m = \frac{1}{A}\int Y dA \qquad (1)$$

where (X^m, Y^m) is the calculated center; the superscript m indicates the iteration number; (X, Y) represents any point that has a reflectivity smaller than a prescribed reflectivity threshold (Z_0) and satisfies

$$(X-X^{m-1})^2 + (Y-Y^{m-1})^2 \le R^2 \qquad (2)$$

A is the total area encompassing all the data points that meets the above two criteria. The radius R is set to R_0 - ΔR in the first iteration, and it increases by 1 km for each new iteration until it reaches R_0 + ΔR or the convergence criteria (defined below in steps 3 and 4) is met.

3) Check if the distance between (X^m, Y^m) and (X^{m-1}, Y^{m-1}) is larger than a pre-specified convergence criterion (α). If yes, then the computation goes back to step 2. The iterative procedure will stop when the convergence condition is met or the iteration number is greater than a threshold (β), or when the radius of computational area, R, reaches its upper limit of $R_0 + \Delta R$.
4) To assure that the derived eye radius encompasses the entire eye region, an additional criterion called "enclosed rate of eye" (ERE) is examined. The ERE is defined as the portion of reflectivity pixels on the boundary of the computed eye that is higher than the pre-specified reflectivity threshold (Z0). If all the pixels on the boundary have weak or no echoes, then it is possible that the computed eye is smaller than the actual eye and the associated ERE is 0. When the ERE is equal to 1.0, it is considered that the computed eye radius has reached the outer edge of the actual eye.
5) Figure 1 illustrates the iterative process of the TCET algorithm. Firstly, an initial guess of the center was made at point A with a radius R_0. Point A is replaced by point B through the procedures (steps 1 to 3) described above.

3. Results and discussions

a. Track

The TCET algorithm was evaluated with 12 typhoon cases (Table 1). These cases included the elliptical eyewall of Typhoon Herb (1996), the concentric eyewall of Dujuan (2003), and Typhoon Nari (2001). The tracking times and distances are also summarized in Table 1. Typhoon Nari (2001) had the longest tracking time of 35 hours. Generally, most typhoons can be tracked for several hours. These well-organized typhoons moved mostly along a westward or south-westward track. Some of them made landfall in Taiwan while others just passed over the sea adjacent to Taiwan (Fig. 2).

Figure 3 shows four examples of typhoons having well-organized eyewall structure as they approached Taiwan. The eye regions were a mixture of echo free and weak reflectivity regions. The Herb eyewall (Fig. 3a) shows an elliptical shape with deep convection near the tip of the major axis. Typhoon Nari (Fig. 3b) exhibited relatively circular-symmetric eyewall structure with some weak echo existing in the eye region. In contrast, both Typhoons Wipha (2007) and Krosa (2007) displayed asymmetric eyewall structures (Figs. 3c and 3d). The eye radius (circles at the domain center, Fig. 3) was about 35 km for Typhoon Herb and about 30 km for Typhoons Nari and Krosa. The smallest eye radius was about 15 km for Typhoon Wipha (Fig. 3c).

b. Track and eye radius comparisons between multiple radars

Since the mean distance between the radars is about 150-200 km in Taiwan's CWB radar network, some TCs [e.g., Typhoon Souderlor (2003) and Shanshan (2006)] were captured by two or even three radars at the same time for several hours. Therefore, comparisons can be made between the TC eye locations and tracks derived from different radars. Figure 4 illustrates the differences between TC center locations derived from RCHL and from two other radars (RCWF and RCKT). The mean difference was about 3.7 km with a standard deviation near 1.5 km. There was a noticeable northern bias, with respect to RCHL, of TC centers derived from RCKT and a southern bias for those from RCWF. As shown in Fig. 2, most of the TC centers were located to the east-northeast of RCHL. If the attenuation of radio wave and outward tilting of the vertical eyewall are considerable, then the TC center locations computed from RCHL would show an eastward bias due to the higher radar beam altitude at the eastern eyewall. Similarly, TC centers derived from RCKT and RCWF should get a northern and a southeastern bias, respectively. The net effect would be a southern (northwestern) bias for TC centers derived from RCWF (RCKT) with respect to those from RCHL.

A comparison between the eye radii derived from RCHL and those from RCWF and RCKT is shown in Fig. 5. Despite of the observations at different ranges from the radar, the derived eye radii showed a high correlation of 0.92. The slope of the linear regression line is 0.99 between the eye radii computed from RCHL and from the two other radars. There was one pair with a difference larger than 10 km in Fig. 5 possibly resulting from observations at significantly different ranges from the radars. Overall, the eye radii derived using TCET from different radars are consistent. This allowed some further investigation of eye radii changes during typhoon landfalls.

c. Changing of eye radius

Figure 6 shows the change of TC eye radius right before TC landfalls as a function of the distance of TC centers to the land (either coastlines of Taiwan or Mainland China). The smallest eye radius was about 4-9 km for Typhoon Dujuan (2003) and the largest was about 67 km for Typhoon Aere (2003). The mean eye radius for 12 typhoons (3257 TC locations) was 25.7 km with a standard deviation of about 11.4 km. The broad distribution of eye radii shown in Fig. 6. The shrinking of eye radii for TCs approaching the land is apparent in Fig. 6, especially for those TCs located within 200 km from the land. However, Typhoon Dujuan was an exception; the small inner eyewall radius remained constant while it passed across the southern tip of Taiwan with a trochoid-like track (Hong and Chang 2005). The similar trend for the change of TC eye radius as a function of distance to the radar is shown in Fig. 7. Owing to the eyewall's outward slope with height, TCs at a greater distance from the radar will likely display larger eye radii than storms closer to the radar. It indicates that the decreasing eye radius as a TC nears landfall may be partially due to decreasing radar-to-eye distance as the storm approaches land. Thus, the contraction of eye radius with decreasing range from land occurs from two possible effects. One is that the TC eyewalls tilt outward with height (Marks et al. 1992). Another is the real contraction of TC eyewalls in nature. The natural contraction effect was shown in Typhoons Saomai (2006) and Wipha (2007), both of which passed over the northern sea area of Taiwan and made landfall at south coast of Mainland China (Fig. 2). At the distances between 250-350 km (close to the Typhoons landfall at the coastlines of Mainland China) from RCWF radar, the eye radius did not increase with increasing range, but instead remained unchanged or even decreased (Fig. 7).

The contraction of the eyewall (eye) is often observed in nature, especially for the hurricanes with concentric eyewalls (Willoughby and Black 1996). The current study found that the contraction occurs when TCs approach land, which is similar to the eyewall contraction of Hurricane Andrew (1992) prior to its landfall at Miami (e.g. Willoughby and Black 1996).

4. Summary

The TCET algorithm is presented to objectively identify the TC eye from radar reflectivity observations. The TCET algorithm is also designed to automatically track the TC center and to compute the eyewall radius when the eyewall is well-organized. Twelve major typhoon cases were analyzed using the TCET algorithm. Sensitivity tests show that the reflectivity threshold and enclosed rate of eye (ERE) are two key parameters for the TCET algorithm. When the ERE is set high, the TCET could fail to identify a center for TCs that have unclosed eyewalls. A high reflectivity threshold could result in an unclosed eyewall, while a too low threshold could result in a small eye region and large

uncertainties in the computed center location. The results from TCET algorithm showed that the longest tracking time was about 35 hours. Further analyses based on the TCET output showed a decrease in the eye size as TCs approach land, especially when the TC center was within 50 km of land.

Generally, the TCET can be applied to determine TC centers for a wide variety of eye and eyewall shapes in radar reflectivity fields (Lewis and Hawkins 1982; Muramatsu 1986; Kuo et al. 1999). But it could fail when the convection band in the eyewall region is too narrow and the ellipticity of the eye region is too high. Therefore, the assumption of a circular eye needs to be modified and expanded to enhance the applications of TCET in future work. The TCET may not accurately find the TC center when a TC is weak or does not have an enclosed eyewall. And the TCET procedure may not work effectively when the storm is undergoing an eyewall replacement cycle or when the outer eyewall is stronger than the inner eyewall, thereby producing gaps in the track. Nevertheless, since the most damaging TCs are usually intense (Pielke and Landsea 1998) and have well-organized eyewall structure, the TCET can be a useful operational tool under these circumstances. Follow-up research will focus on techniques that integrate contractions, intensities and intensity changes for landfalling TCs. information about center locations, tracks, eyewall Doppler velocity and reflectivity to provide more accurate

Acknowledgements: The authors would like to thank Central Weather Bureau for providing the radar data and computer resources. This research is supported by the National Science Council of Taiwan, Republic of China, under Grant 96-2625-Z-052-005-.

Reference

Blackwell, K. G. 2000: The Evolution of Hurricane Danny (1997) at Landfall: Doppler-Observed Eyewall Replacement, Vortex Contraction /Intensification, and Low-Level Wind Maxima.*Mon. Wea. Rev.*, **128**, 4002–4016.

Chang, P. –L., B. J. -D. Jou, and J. Zhang, 2008: An Algorithm for Tracking Eyes of Tropical Cyclones. *Wea. Forecasting*. (Accepted for publication).

Griffin, J. S., R. W. Burpee, F. D. Marks, Jr., and J. L. Franklin, 1992: Real-time airborne analysis of aircraft data supporting operational hurricane forecasting. *Wea. Forecasting*, **7**, 480-490.

Kuo, H. C., R. T. Williams, and J. H. Chen, 1999: A possible mechanism for the eye rotation of Typhoon Herb. *J. Atmos. Sci.*, **56**, 1659–1673.

Lee, W.-C., and F. D. Marks, 2000: Tropical cyclone kinematic structure retrieved from single Doppler radar observations. Part II: The GBVTD-simplex center finding algorithm. *Mon. Wea. Rev.*, **128**, 1925–1936.

——, B. J.-D. Jou, P. -L. Chang, and S. -M. Deng, 1999: Tropical cyclone kinematic structure retrieved from single Doppler radar observations. Part I: Interpretation of Doppler velocity patterns and the GBVTD technique. Mon. Wea. Rev., 127, 2419–2439.

Lewis, B. M., and H. F. Hawkins, 1982: Polygonal eye walls and rainbands in hurricanes. *Bull. Amer. Meteor. Soc.*, **63**, 1294–1300.

Marks, F. D., Jr., R. A. Houze, and J. Gamache, 1992: Dual-aircraft investigation of the inner core of Hurricane Norbert: Part I: Kinematic structure. *J. Atmos. Sci.*, **49**, 919-942.

Muramatsu, T., 1986: The structure of polygonal eye of a typhoon. *J. Meteor. Soc. Japan*, **64**, 913-921.

Parrish, J. R., R. W. Burpee, F. D. Marks, Jr., and C. W. Landsea, 1984: Mesoscale and convective-scale characteristics of Hurricane Frederic during landfall. Postprints, *15th Conf. on Hurricanes and Tropical Meteorology*, Miami, FL, Amer. Meteor. Soc., 415–420.

Pielke, R. A., Jr., and C. W. Landsea, 1998: Normalized hurricane damages in the United States: 1925–95. *Wea. Forecasting*, **13**, 621–631.

Willoughby H. E., 1998: Tropical cyclone eye thermodynamics. *Mon. Wea. Rev.*, **126**, 1653–1680.

——, and P. G. Black, 1996: Hurricane Andrew in Florida: Dynamics of a disaster. *Bull. Amer. Meteor. Soc.*, **77**, 543-549.

Wood, V. T., and R. A. Brown, 1992: Effects of radar proximity on single-Doppler velocity signatures of axisymmetric rotation and divergence. *Mon. Wea. Rev.*, **120**, 2798-2807.

Wu, C.-C., T. -H. Yen, Y. -H. Kuo, and W. Wang, 2002 : Rainfall simulation associated with Typhoon Herb (1996) near Taiwan. Part I: The topographic effect. *Wea. Forecasting*, **17**, 1001-1015

TABLE 1. Typhoon cases selected for TCET analysis. The dash symbols in tracking duration indicate no data available from the listed radar.

	Typhoon Names	Date	Radars Tracked	Tracking Duration (hrs)			Landfall ?
				RCWF	RCHL	RCKT	
1	Herb (1996)	July 30-31	1	15.6	-	-	Yes
2	Nari (2001)	September 15-16	1	35.7	-	-	Yes
3	Soudelor (2001)	June 17-18	3	13.0	2.8	14.0	No
4	Dujuan (2003)	September 01	1	-	-	13.3	No
5	Aere (2004)	August 24-25	1	25.7	-	-	No
6	Haitang (2005)	July 17	2	14.2	15.2	-	Yes
7	Longwang (2005)	October 1	3	12.9	16.4	8.7	Yes
8	Saomai (2006)	August 09-10	2	24.1	7.0	-	No
9	Khanun (2006)	September 10-11	2	21.4	15.7	-	No
10	Shanshan (2006)	September 14-16	3	23.0	24.8	25.5	No
11	Wipha (2007)	September 17-18	2	30.3	19.3	-	No
12	Krosa (2007)	October 05-07	3	14.5	17.7	9.2	Yes

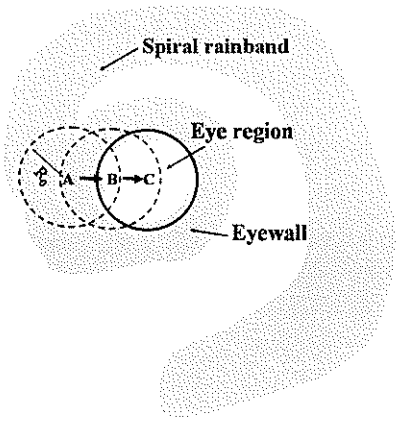

FIG. 1. The schematic diagram of the TCET convergence path. The calculations start with initial center location A and radius R_0. Points B and C indicate the new centers computed from iterations. Grey areas depict where the reflectivity is above the threshold Z_0.

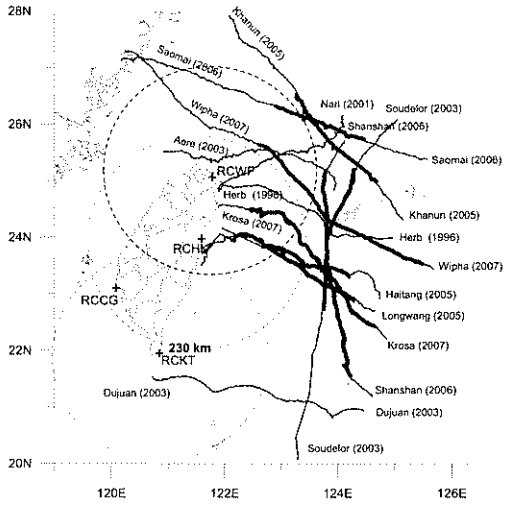

FIG. 2. Typhoon tracks determined by the TCET algorithm. The grey lines indicate tracks from the TCET algorithm and heavy solid lines represent the tracks determined from two or three radars at the same time. The radar sites are labeled with "+" symbols. Range rings of 230 km centered at each radar site are also indicated.

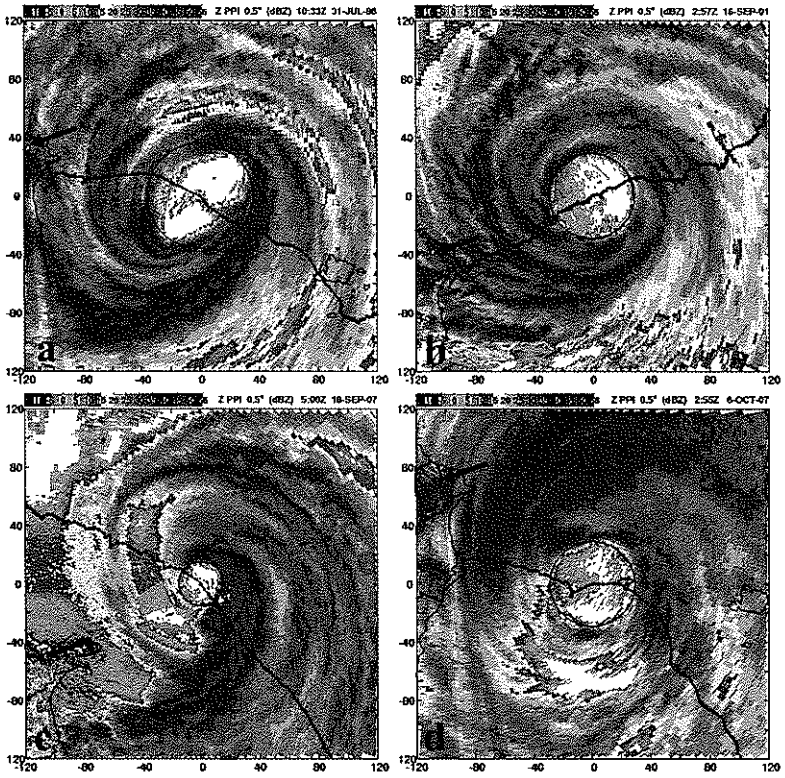

FIG. 3. RCWF base reflectivities at 0.5° elevation from (a) Typhoon Herb at 1033 UTC on 31 July 1996, (b) Typhoon Nari at 0257 UTC on 16 September 2001, (c) Typhoon Wipha at 0500 UTC on 18 September 2007 and (d) Typhoon Krosa 0255 UTC on 6 October 2007. The Typhoon tracks (blue lines) are overlaid with the radar reflectivity for each 240 km x 240 km domain. The blue solid circles indicate inner eye boundaries determined by the TCET algorithm. The RCWF radar site is indicated by the black arrow.

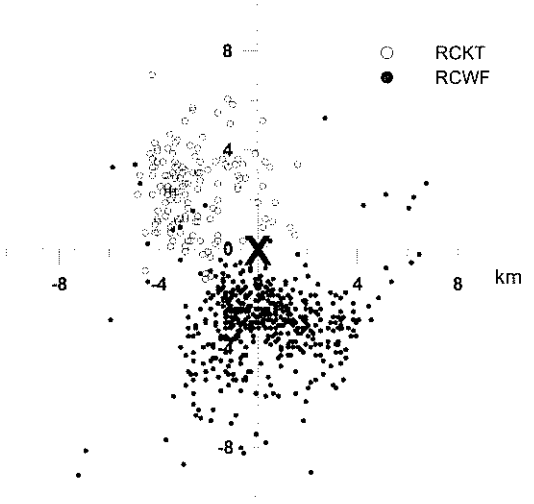

FIG. 4. Differences (km) between the TC center locations derived from RCHL and from 1) RCWF (filled circle) and 2) RCKT (open circle) radars. The location differences are displayed with the RCHL radar ("X" point) as the reference point.

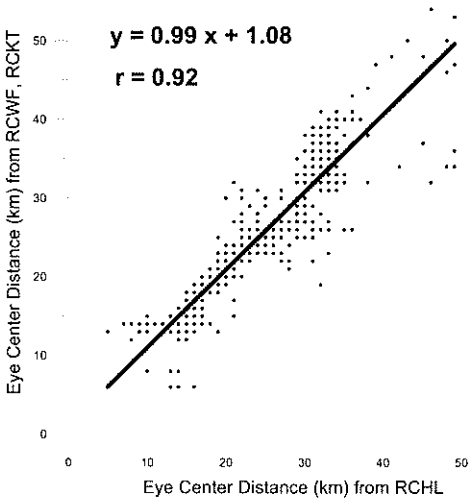

FIG. 5. Scatterplot of eye radii (km) computed from RCHL and from RCWF and RCKT. The correlation coefficient is 0.92 and the equation of linear regression is indicated.

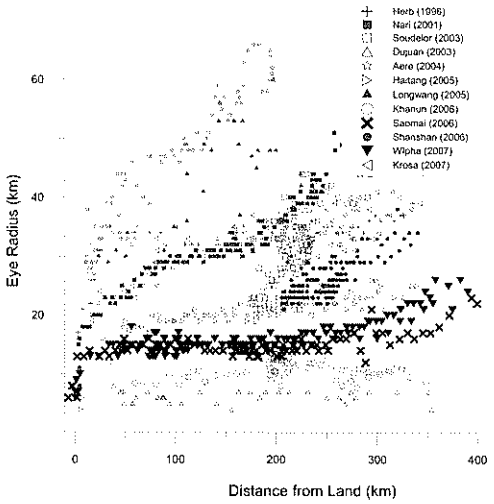

FIG. 6. Eye radii of TCs as a function of the distance of TC centers to land for selected Typhoons.

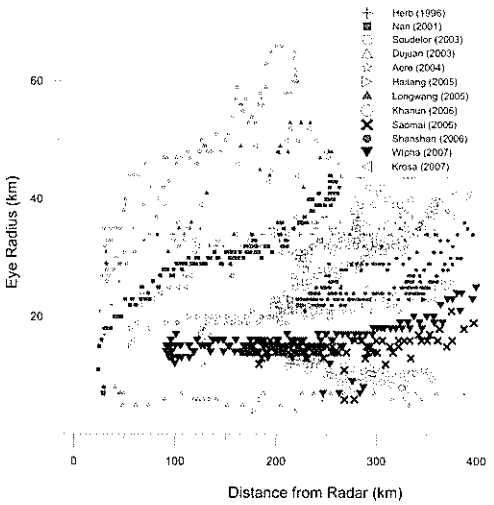

FIG. 7. Eye radii of TCs as a function of the distance of TC centers to radars for selected Typhoons.